


Control of Surface Chemical Reactions through Solid Stiffness

Jianqi Xi¹ and Izabela Szlufarska^{1,2,*}

¹*Department of Materials Science and Engineering, University of Wisconsin, Madison, Wisconsin 53706, USA*

²*Department of Engineering Physics, University of Wisconsin, Madison, Wisconsin 53706, USA*

 (Received 29 January 2022; revised 14 August 2022; accepted 17 August 2022; published 2 September 2022)

Control of surface reactions is commonly achieved by modification of surface electronic structures. Here, we discover an alternative pathway for controlling surface reactions by tuning the mechanical stiffness of the underlying material. We find that in addition to the typically assumed surface electronic contribution right at the reactive site, the contribution from the deformation of the bulk region plays a vital role in controlling surface reactions. The underlying mechanism is an elastic relaxation of the solid, which depends on the material's stiffness and can be modified by tuning bulk stoichiometry. The effect of bulk stiffness on surface reactions has been demonstrated by considering hydrogen scission reaction and oxygen incorporation reaction during corrosion of amorphous SiC in water and air, respectively. Our results imply that tuning of bulk stiffness by modifying stoichiometry can provide an effective method for controlling surface reactions.

DOI: [10.1103/PhysRevLett.129.106101](https://doi.org/10.1103/PhysRevLett.129.106101)

Surface reactions are at the heart of many technical fields, such as corrosion of structural materials, electrochemical conversion of exhaust gases, etc. Corrosion can cause dangerous and expensive damage to everything from automobiles, bridges, and even power plants [1–3], whereas electrolysis plays an important role in the reduction of CO₂ emission [4,5], and Li-ion batteries promise for high-performance electrochemical energy storage [6,7]. It is not surprising that in the past decades, multiple efforts to control surface reactions have been reported. One effective way is by tuning surface structure [8–14]. For example, studies of metallic nanoparticles have shown that the surface catalytic performance of the nanoparticles can be dramatically enhanced by increasing low-coordinated surface steps [11–13], stretching surface lattice [8,10,11], and densifying defects on the surface [10,13,14]. These particular surface engineering approaches have been widely employed in materials with transition metals, and the strategy is supported by an underpinning theory, i.e., a surface “*d*-band model” [8,14]. In this model, the interaction between the adsorbates and metallic atoms on the surface is determined by the energy level of the surface *d*-band center. The higher the energy of the surface *d*-band center is relative to the Fermi energy, the stronger the interaction with adsorbates. Engineering of surface reactivity by modifying surface electronic structure has also been employed in materials without transition metals, such as the hydrogen passivation of silicon to suppress surface activity [15,16] and the functionalization of the silicon carbide surface to control hydrophobicity [17,18]. In addition to the solid surface engineering, surface reactions can be controlled by modifying the environment, e.g., in the case of a liquid solution in contact with the solid surface,

by controlling the *pH* and impurity ions in the solution [19–21]. For example, *pH* has been used effectively to control the electrochemical dehydrogenation rate on silica surfaces [20,21].

All the above efforts mainly focus on modifications of solid surface electronic states right at the reactive site, which is generally assumed to control the surface reaction. Interestingly, it has been recently shown that in addition to surface structure and environment, reaction rates could be impacted by the bulk properties of the solid if the solid is subjected to mechanical stress or strain. This kind of mechan-chemical coupling has been found during chemisorption on the surface of biaxially strained transition metal systems, especially if they contained stepped surfaces [22], and during reactions of silanol groups at silica-silica interfaces under compressive stress [23]. While it might be not as surprising that surface properties of a solid change when the solid is subjected to strain, these studies raise the question of the impact of bulk properties on surface reactions in general. As explained above, up until now in stress-free materials surface reactions have been generally expected to depend primarily on the surface properties and environment.

Here, we demonstrate that contrary to what had been previously assumed, surface reactions in stress-free materials can in fact have a strong dependence on the bulk properties of a solid. Specifically, we find that there is a significant contribution to surface reactions from the mechanical relaxation of the underlying solid, which is mainly controlled by the intrinsic stiffness of the material. These conclusions are based on a series of quantum mechanical calculations of chemical reactions underlying environmental degradation of stress-free amorphous SiC

(*a*-SiC). We demonstrate the impact of bulk stiffness on surface reactivity using a specific example of hydrogen scission reaction, which is a key step in the hydrothermal corrosion of SiC [24,25]. To verify our predictions, we have carried out additional studies of the oxygen incorporation reaction, which is a critical step during oxidation of SiC in air [26] (see Supplemental Material [27]). Energetics of both types of chemical reactions were found to have the same qualitative dependence on the bulk properties of SiC. We chose *a*-SiC as a model material, as its surface reactivity is relevant to a number of fields, such as the membrane materials in micro- and nano-electromechanical (MEM and NEM) device applications [40], membranes for microfluidic devices [41], and fabrication of polycrystalline materials in which the highly disordered grain boundaries have a resemblance and are commonly regarded as *a*-SiC regions [42]. In addition, the choice of *a*-SiC offers the added flexibility of tuning the physical properties of solids by adjusting the C/Si stoichiometry, allowing the realization of materials with properties that span those of *a*-Si and *a*-C. In this Letter, to study the effect of the properties of the solid on surface reactions, we have considered three *a*-SiC systems with different bulk stoichiometries, corresponding to the C/Si ratios of 0.8 (C-rich), 1.0 (stoichiometric), and 1.2 (Si-rich). Simulation details are provided in the Supplemental Material [27].

Environmental degradation of crystalline SiC in high-temperature water is known to be accomplished mechanically by the attack of Si—C surface bonds by H, called a hydrogen scission reaction. The H atom is first emitted from a hydroxyl group previously adsorbed on the surface. The hydrogen scission reaction results in C being passivated by H atoms, and surface Si becoming hydroxylated [24,25]. In simple terms, subsequent H scission reactions enable further hydroxylation of Si, which eventually is released into the water as Si(OH)₄. C initially forms a C-rich layer on the SiC surface and eventually it is dissolved as gas phases [43]. The H scission reaction is thus a key mechanism that drives environmental degradation of crystalline SiC in high-temperature water. Here, using *ab initio* molecular dynamics (AIMD) we have confirmed that the hydrogen scission reaction plays the same role in breaking Si—C bonds during degradation of *a*-SiC (see Fig. S3 [27]). Estimating the reaction energy of hydrogen scission on *a*-SiC surface is complicated by the structural disorder and the limited number of reactions observed within the AIMD simulations. Therefore, to find the possible energy distribution of hydrogen scission reactions in *a*-SiC with different stoichiometries, we artificially displaced the hydrogen atom from the hydroxyl group adsorbed to Si (i.e., Si—OH group) toward a Si—C surface bond. Minimizing the total energy of 60 independent samples with respect to different atomic coordinates shows that in these positions the hydrogen scission can only occur for those surface Si—C bonds that are longer

than ~ 1.889 Å. Once the hydrogen scission occurred, the dangling bond in the undercoordinated Si—O group that remains on the surface can be spontaneously passivated by another H atom that comes from the surrounding water molecule. Specifically, a water molecule around the reactive site is dissociated into —H and —OH, and the H atom tends to passivate the undercoordinated Si—O group, while the —OH is adsorbed onto the surface and binds to a Si atom near the reactive site.

Figure 1 shows the calculated reaction energies for the aforementioned H scission reactions in *a*-SiC with different stoichiometries. We find that the reaction energy is highly dependent on the bulk stoichiometry of *a*-SiC. Generally, the reaction energies on the surfaces of stoichiometric and Si-rich systems are negative, meaning that the hydrogen scission reaction is energetically favorable to occur on those surfaces. The reaction energies in a Si-rich system (from -0.229 to -1.171 eV) are slightly smaller than those in stoichiometric system (from -0.006 to -0.771 eV), suggesting that the presence of additional Si atoms in *a*-SiC can moderately reduce the hydrogen scission reaction energy. The most dramatic effect can be seen on the surface of a C-rich system, where the reaction energies are significantly increased and become positive, ranging from -0.058 to 0.922 eV. We note that we have observed another type of reaction on the surface of the C-rich system, i.e., once the H atoms are emitted from the Si—OH group, the dangling bond in the Si—O group remaining on the surface is not repassivated. These reactions occur because the excess carbon atoms that exist on the surface can form a C—C chain structure around the reactive site (see Fig. S5 [27]). Such structure suppresses dissociation of a nearby H₂O because the strong C—C bond makes the electrostatic interaction between the C—C structure and H₂O molecule negligible. This behavior qualitatively resembles the adsorption of H₂O on the diamond surface [44] and on the C-terminated surface of SiC [17,18]. In this case, the energy for hydrogen scission reaction is higher than ~ 1.0 eV, which means that this scenario is

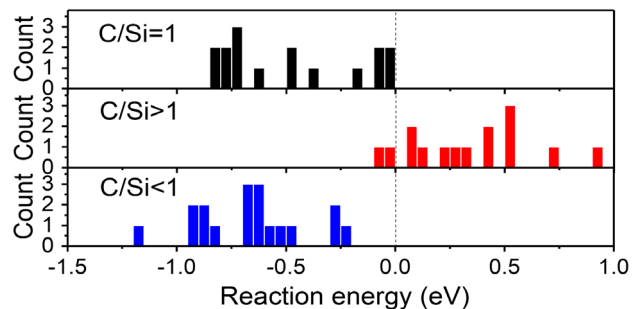


FIG. 1. Distribution of reaction energy for the hydrogen scission reaction in *a*-SiC with different stoichiometric conditions. Here C/Si = 1, >1, and <1 represent the stoichiometric, C-rich, and Si-rich systems, respectively.

thermodynamically difficult to occur. The increase in reaction energies on C-rich surfaces was also found for reactions involving oxygen gas adsorption and incorporation on the *a*-SiC surfaces (see Supplemental Material [27]). Finally, as described by the Bronsted-Evans-Polanyi relation [45], the reaction energy is often linearly correlated with the activation energy barrier. This linear relation for the hydrogen scission reaction on SiC has been confirmed by our previous DFT calculations [25]. Therefore, the current results suggest that tuning of bulk stoichiometry of *a*-SiC with high carbon contents can increase the surface reaction energy barriers and therefore decrease the surface reaction rate.

To understand the origin of the above effect of stoichiometry on the hydrogen scission reaction, we have isolated the contributions to the reaction energy from the electron redistribution at the surface reactive sites (electronic contribution to reaction energy) and from the elastic relaxation in the surrounding bulk region (bulk contribution to the reaction energy).

The electronic contribution, ΔE_{ele} , was evaluated by considering the energy cost associated with the changes in chemical bonding states right at the reactive site (involving the H scission of the Si—C bond and the subsequent passivation reactions at the reactive site). Because of the complexity of the reaction processes, we decomposed the changes in chemical bonding states during the hydrogen scission reaction into four steps shown in Fig. 2(a). These are (i) ΔE_{ele}^1 , breaking of the O—H bond in the surface Si—OH group, while holding positions of all the ions in

both the *a*-SiC substrate and the H₂O solution fixed in the configuration before reaction; $\Delta E_{\text{ele}}^1 = E(\text{SiO}) + \mu(\text{H}) - E(\text{SiOH})$, where $E(\text{Si—OH})$ and $E(\text{Si—O})$ are the energies of system with adsorbed Si—OH group before and after emitting H, respectively. $\mu(\text{H})$ is the chemical potential of hydrogen atom; (ii) ΔE_{ele}^2 , incorporation of H atom to form C—H bond, while fixing the ions in both the substrate and solution in the configuration after reaction; $\Delta E_{\text{ele}}^2 = E(\text{CH}) - \mu(\text{H}) - E(\text{C})$, where $E(\text{C—H})$ and $E(\text{C})$, respectively, are the energies of system with and without H passivation to form C—H bond; (iii) $\Delta E_{\text{ele}}^{32}$, breaking of the Si—C bond due to H incorporation, which is estimated by calculating the bond strength of Si—C bond before reaction (see Supplemental Material [27]); (iv) ΔE_{ele}^4 , dissociation of a nearby H₂O to passivate the dangling bond in the Si—O group that remained on the surface after emitting of H atom. In the H₂O dissociation process, positions of ions in the *a*-SiC substrate are fixed, while water molecules and the adsorbates at the reactive site are fully relaxed. In above steps, the electron redistributions have been fully considered. The electronic contribution can be then estimated as the sum of the energy costs in above steps, i.e., $\Delta E_{\text{ele}} = \sum_i^4 \Delta E_{\text{ele}}^i$. Here, we should note that dividing the reaction into four steps is necessary in order to consider the energy change along the actual reaction path. There is electronic energy lost or gained along the path, so the total contribution along the reaction path is not equal to the difference between the final and the initial state. From Fig. 2(b), one can see that the energy cost due to the

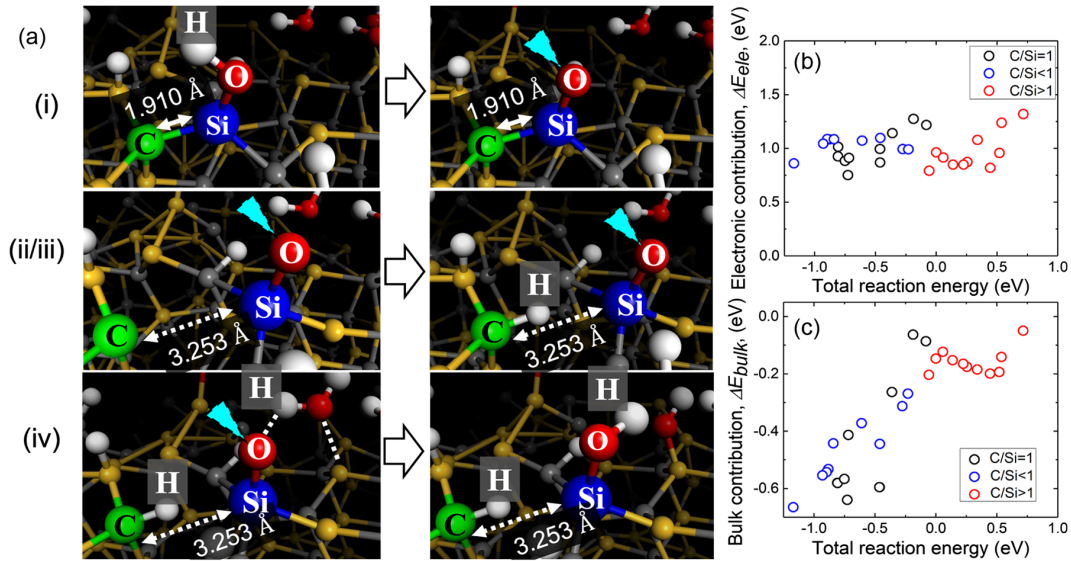


FIG. 2. (a) Steps of chemical bond breaking and formation during a hydrogen scission reaction: (i) breaking of O—H bond in the surface Si—OH group; (ii) and (iii) breaking of C—Si bond and formation of C—H bond due to the hydrogen scission and incorporation; (iv) passivation of Si—O due to the dissociation of H₂O around the reactive site. The yellow spheres are the silicon atoms, gray ones are the carbon atoms, red ones are the oxygen atoms, and white ones are the hydrogen atoms; the large blue and green spheres are the silicon and carbon atoms right at the reactive site, respectively. (b) and (c) Electronic and bulk contributions to the hydrogen scission reaction as a function of total reaction energy, respectively.

changes in chemical bonding states at the reactive site is largely independent of stoichiometry.

Our AIMD simulations reveal that when a hydrogen scission reaction occurs, it results in displacements of atoms in the substrate. Specifically, the incorporation of the H atom to break the Si—C surface bond will displace Si and C atoms right at the reactive site, which allows their surrounding atoms to move away from the reactive site and causes the relaxation of surrounding solids. The bulk relaxation, ΔE_{bulk} , can release the mechanical energy in the solid induced by the surface reaction, and thus reduce the reaction energy. To evaluate the change in the mechanical energy caused by H scission reaction, we removed from the simulation cells all the H_2O molecules in the solution as well as adsorbates (both before and after the reaction). Additionally, to exclude from the calculations of energy associated directly with the breaking of the Si—C bond at the reactive site, we removed those Si and C atoms that participate in the broken Si—C bond at the reactive site, and then passivated the remaining dangling bonds with hydrogens both before and after the reaction. The same number of molecules and atoms was removed or added in the systems before and after the reaction. Finally, we calculated the total energy difference of the systems before and after the reaction. Since elastic deformation is a reversible process, the amount of elastic relaxation does not depend on the reaction path, and thus can be calculated as the difference between the initial and final state. Generally, the more negative change in the mechanical energy, the more relaxation occurs, which makes the reaction energetically more favorable. We note that in C-rich and Si-rich systems, there might be C—C or Si—Si bonds present near the reactive site, meaning that the local chemical environment is different from the stoichiometric systems. The different local chemistry environments can induce different mechanical relaxation. To eliminate the effect of the local chemistry on the solid mechanical energy, in our comparison between different systems we only included those cases of reactions where there were no homonuclear (C—C or Si—Si) bonds present right near the reactive site.

As shown in Fig. 2(c), changes in the mechanical energy caused by hydrogen scission reaction have a strong dependence on bulk stoichiometry. For a C-rich system, the magnitude of the change in the mechanical energies, $|\Delta E_{\text{bulk}}|$, around different reactive sites are almost constant and not larger than 0.2 eV, indicating that the bulk relaxation contribution to the reaction energy in a C-rich system is minor. This is consistent with the negligible changes of Si—C bond length distributions before and after reaction, as shown in Fig. 3(a). The changes in the mechanical energy for stoichiometric and Si-rich systems are significantly larger than those found in a C-rich system, and the value ranges from -0.063 to -0.665 eV [see Fig. 2(c)]. This trend is consistent with the more

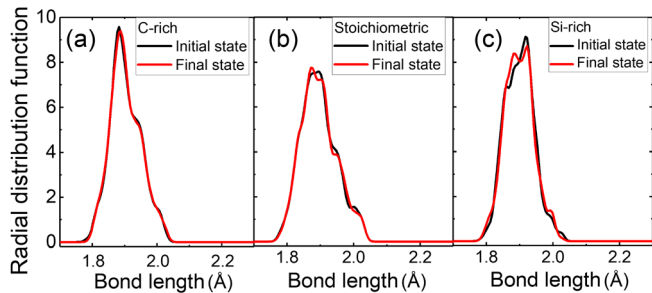


FIG. 3. The averaged radial distribution function of Si—C bond in systems with different stoichiometries before (initial state) and after (final state) hydrogen scission reaction.

pronounced changes in the Si—C bond length distribution in stoichiometric and Si-rich α -SiC than in a C-rich system (see Fig. 3). The same qualitative dependence of changes in the mechanical energy on stoichiometry was found for the oxygen incorporation reaction on α -SiC surfaces (see Fig. S2 [27]).

By comparing Figs. 2(b) and 2(c), we can conclude that the major contribution to the variation of surface reaction energy in systems with different stoichiometries (see Fig. 1) comes from the changes in the mechanical energy of the surrounding solid, rather than from the changes in the electronic energy associated with broken surface bonds. This is because the changes in the electronic energy at the reactive sites in these systems are relatively constant and therefore independent of the total reaction energy. The reaction energies generally decrease as the change in the mechanical energy becomes more negative, corresponding to a stronger driving force from the elastic relaxation. This trend is particularly evident in stoichiometric and Si-rich systems [Fig. 2(c)]. It should be noted that although the magnitude of the change in the electronic energy is larger than that of the mechanical energy, the sum of these two contributions has a similar trend as the change in the mechanical energy (see Fig. S7 [27]), which means that the mechanical energy dominates the total reaction energy. These results suggested that the contribution from elastic relaxation of solids plays an important, and in some cases dominant, role in the energetics of surface chemical reactions.

In a hydrogen scission reaction, the incorporation of a H atom into the surface Si—C bond can induce local stress into the solid to displace the Si and C atoms at the reactive site. Because of the comparable bond length and bond strength of the surface Si—C bond, the reaction-induced stresses should be comparable in the systems with different stoichiometries (see Supplemental Material [27]). Therefore, in the absence of plastic deformation, the resistance to mechanical relaxation can be directly attributed to the mechanical stiffness of material, i.e., the stiffer of the material, the smaller its relaxation. We have calculated the stiffnesses of α -SiC samples and they are

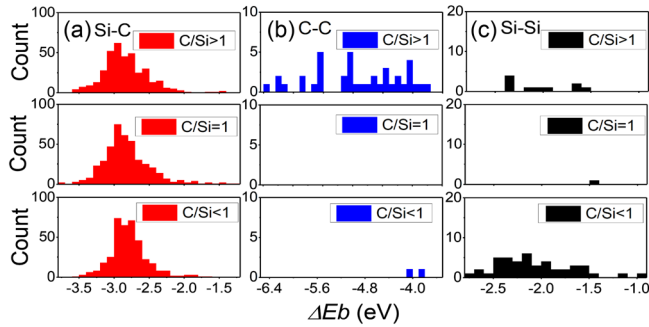


FIG. 4. Bond population and bond strength distribution for Si–C, C–C, and Si–Si bonds in *a*-SiC with different stoichiometries.

listed in Table S2 [27]. These data show that the elastic stiffnesses of *a*-SiC increase with increasing carbon content, which is consistent with previous experimental measurements [46,47]. This is understandable since the elastic stiffness of a material can be attributed to the strength of its chemical bonds, i.e., the stronger the chemical bond, the larger the elastic stiffness. As shown in Fig. 4, the bond strength in *a*-SiC follows the order of $\Delta E_b(\text{C-C}) > \Delta E_b(\text{Si-C}) > \Delta E_b(\text{Si-Si})$. For C-rich *a*-SiC, its average bond strength is much larger than that of stoichiometric and Si-rich systems, due to the existence of a large number of homonuclear C–C bonds. The Si-rich *a*-SiC has the lowest elastic modulus, which results from the presence of weaker Si–Si bonds.

In summary, we have shown that tuning bulk stiffness by changing bulk stoichiometry can be an effective tool for controlling surface reactions. For materials with lower stiffness, such as stoichiometric and Si-rich *a*-SiC, relaxation in solid can release the stored mechanical energy induced by the reaction in the substrate, and thus reduce the reaction energy. For stiffer materials, such as C-rich *a*-SiC, the formation of large amounts of stronger C–C bonds dramatically enhances the mechanical stiffness of material, so that the mechanical relaxation in the bulk region can be negligible, and the surface reaction energies in C-rich system are generally higher than those in stoichiometric and Si-rich ones. The ability to tailor surface reactions via bulk mechanical stiffness has potential impact on the design of materials with respect to such phenomena as corrosion, electrochemical energy storage, and friction, etc. Finally, our results provide new insights into degradation mechanisms of SiC, which is an important material for future energy systems.

From the practical perspective, the stoichiometry of the materials could be changed either in the sample preparation process [48–50] or by other postprocessing phenomena such as radiation-induced segregation [51]. For instance, irradiation experiments in polycrystalline SiC have shown that there is irradiation-induced segregation of C to high-energy grain boundaries [51], which often have highly

disordered amorphous-like structures. Our results suggest that irradiation could suppress grain boundary corrosion under circumstances where such radiation-induced segregation takes place.

The authors gratefully acknowledge support from Department of Energy Basic Energy Science Program (Grant No. DEFG02-08ER46493).

*szlufarska@wisc.edu

- [1] T. Allen, J. Busby, M. Meyer, and D. Petti, *Mater. Today* **13**, 14 (2010).
- [2] X. Li, D. Zhang, Z. Liu, Z. Li, C. Du, and C. Dong, *Nature (London)* **527**, 441 (2015).
- [3] Y. Xie, D. M. Artymowicz, P. P. Lopes, A. Aiello, D. Wang, J. L. Hart, E. Anber, M. L. Taheri, H. Zhuang, R. C. Newman, and K. Sieradzki, *Nat. Mater.* **20**, 789 (2021).
- [4] W. Weng, B. Jiang, Z. Wang, and W. Xiao, *Sci. Adv.* **6**, eaay9278 (2020).
- [5] S. Licht, *Adv. Mater.* **23**, 5592 (2011).
- [6] X. He *et al.*, *Nat. Rev. Mater.* **6**, 1036 (2021).
- [7] J. M. Tarascon and M. Armand, *Nature (London)* **414**, 359 (2001).
- [8] M. Mavrikakis, B. Hammer, and J. K. Nørskov, *Phys. Rev. Lett.* **81**, 2819 (1998).
- [9] L. P. Wolters and F. M. Bickelhaupt, *Comput. Mol. Sci.* **5**, 324 (2015).
- [10] S. A. Akhade and J. R. Kitchin, *J. Chem. Phys.* **137**, 084703 (2012).
- [11] S. Schnur and A. Groß, *Phys. Rev. B* **81**, 033402 (2010).
- [12] L. Luo, L. Li, D. K. Schreiber, Y. He, D. R. Baer, S. M. Brummer, and C. Wang, *Sci. Adv.* **6**, 1 (2020).
- [13] Q. Zhu, Z. Pan, Z. Zhao, G. Cao, L. Luo, C. Ni, H. Wei, Z. Zhang, F. Sansoz, and J. Wang, *Nat. Commun.* **12**, 558 (2021).
- [14] J. K. Nørskov, T. Bligaard, J. Rossmeisl, and C. H. Christensen, *Nat. Chem.* **1**, 37 (2009).
- [15] Z.-H. Wang, T. Urisu, S. Nanbu, J. Maki, G. Ranga Rao, M. Aoyagi, H. Watanabe, and K. Ooi, *Phys. Rev. B* **69**, 045309 (2004).
- [16] M. K. Weldon, B. B. Stefanov, K. Raghavachari, and Y. J. Chabal, *Phys. Rev. Lett.* **79**, 2851 (1997).
- [17] G. Cicero, J. C. Grossman, A. Catellani, and G. Galli, *J. Am. Chem. Soc.* **127**, 6830 (2005).
- [18] G. Cicero, A. Catellani, and G. Galli, *Phys. Rev. Lett.* **93**, 016102 (2004).
- [19] K. Leung, I. M. B. Nielsen, and L. J. Criscenti, *J. Am. Chem. Soc.* **131**, 18358 (2009).
- [20] M. Sulpizi, M. P. Gageot, and M. Sprik, *J. Chem. Theory Comput.* **8**, 1037 (2012).
- [21] K. Leung, L. J. Criscenti, A. W. Knight, A. G. Ilgen, T. A. Ho, and J. A. Greathouse, *J. Phys. Chem. Lett.* **9**, 5379 (2018).
- [22] M. F. Francis and W. A. Curtin, *Nat. Commun.* **6**, 6261 (2015).
- [23] Z. Li and I. Szlufarska, *Phys. Rev. Lett.* **126**, 076001 (2021).
- [24] J. Xi, C. Liu, D. Morgan, and I. Szlufarska, *Acta Mater.* **209**, 116803 (2021).

- [25] J. Xi, C. Liu, D. Morgan, and I. Szlufarska, *J. Phys. Chem. C* **124**, 9394 (2020).
- [26] M. Di Ventra and S. T. Pantelides, *Phys. Rev. Lett.* **83**, 1624 (1999).
- [27] See Supplemental Material at <http://link.aps.org/supplemental/10.1103/PhysRevLett.129.106101> for additional discussions about computational methods, details of surface chemical reactions, and other discussions, which includes Refs. [24,25,28–39].
- [28] I. Szlufarska, R. K. Kalia, A. Nakano, and P. Vashishta, *J. Appl. Phys.* **102**, 023509 (2007).
- [29] S. Plimpton, *J. Comput. Phys.* **117**, 1 (1995).
- [30] P. Vashishta, R. K. Kalia, A. Nakano, and J. P. Rino, *J. Appl. Phys.* **101**, 103515 (2007).
- [31] J. Xi, G. Bokas, L. E. Schultz, M. Gao, L. Zhao, Y. Shen, J. H. Perepezko, D. Morgan, and I. Szlufarska, *Comput. Mater. Sci.* **185**, 109958 (2020).
- [32] G. Kresse and J. Furthmüller, *Phys. Rev. B* **54**, 11169 (1996).
- [33] G. Kresse and D. Joubert, *Phys. Rev. B* **59**, 1758 (1999).
- [34] J. P. Perdew, K. Burke, and M. Ernzerhof, *Phys. Rev. Lett.* **77**, 3865 (1996).
- [35] S. Grimme, *J. Comput. Chem.* **27**, 1787 (2006).
- [36] Volker L. Deringer, A. L. Tchougreff, and R. Dronskowski, *J. Phys. Chem. A* **115**, 5461–5466 (2011).
- [37] D. H. Tsai, *J. Chem. Phys.* **70**, 1375 (1979).
- [38] Y. Cui and H. B. Chew, *J. Chem. Phys.* **150**, 144702 (2019).
- [39] M. Yu, D. R. Trinkle, and R. M. Martin, *Phys. Rev. B* **83**, 115113 (2011).
- [40] N. Ledermann, J. Baborowski, P. Murali, N. Xantopoulos, and J. M. Tellenbach, *Surf. Coat. Technol.* **125**, 246 (2000).
- [41] D. S. Wu, R. H. Horng, C. C. Chan, and Y. S. Lee, *Appl. Surf. Sci.* **144–145**, 708 (1999).
- [42] F. Cancino-Trejo, E. López-Honorato, R. C. Walker, and R. S. Ferrer, *J. Nucl. Mater.* **500**, 176 (2018).
- [43] C. H. Henager, A. L. Schemer-Kohrn, S. G. Pitman, D. J. Senor, K. J. Geelhood, and C. L. Painter, *J. Nucl. Mater.* **378**, 9 (2008).
- [44] Y. Okamoto, *Phys. Rev. B* **58**, 6760 (1998).
- [45] M. G. Evans and M. Polanyi, *Trans. Faraday Soc.* **34**, 11 (1938).
- [46] Q. Zhao, Z. Zhang, Y. Li, and X. Ouyang, *RSC Adv.* **7**, 28499 (2017).
- [47] M. A. El Khakani, M. Chaker, A. Jean, S. Boily, J. C. Kieffer, M. E. O’Hern, M. F. Ravet, and F. Rousseaux, *J. Mater. Res.* **9**, 96 (1994).
- [48] A. Majid, *Ceram. Int.* **44**, 1277 (2018).
- [49] K. Xue, L. S. Niu, H. J. Shi, and J. Liu, *Thin Solid Films* **516**, 3855 (2008).
- [50] M. Kuenle, S. Janz, O. Eibl, C. Berthold, V. Presser, and K. G. Nickel, *Mater. Sci. Eng. B.* **159–160**, 355 (2009).
- [51] X. Wang, H. Zhang, T. Baba, H. Jiang, C. Liu, Y. Guan, O. Elleuch, T. Kuech, D. Morgan, J. C. Idrobo, P. M. Voyles, and I. Szlufarska, *Nat. Mater.* **19**, 992 (2020).